Diversity-multiplexing tradeoff in mode-division multiplexing

Sercan Ö. Arık* and Joseph M. Kahn

E. L. Ginzton Laboratory, Department of Electrical Engineering, Stanford University, Stanford, California 94305, USA
**Corresponding author: soarik@stanford.edu*

Received January 21, 2014; revised March 27, 2014; accepted April 16, 2014;
posted April 16, 2014 (Doc. ID 205253); published May 27, 2014

The capacity of mode-division multiplexing (MDM) systems is limited, for a given outage probability, by mode-dependent loss (MDL) and gain. Modal degrees of freedom may be exploited to increase transmission rate (multiplexing gain) or lower outage probability (diversity gain), but there is a fundamental tradeoff between the achievable multiplexing and diversity gains. In this Letter, we present the diversity-multiplexing tradeoff in MDM systems for the first time, studying the impact of signal-to-noise ratio, MDL, and frequency diversity order on the tradeoff in the strong-mode-coupling regime.

OCIS codes: (060.2330) Fiber optics communications; (060.4230) Multiplexing; (060.4510) Optical communications.
http://dx.doi.org/10.1364/OL.39.003258

The sustained exponential growth of data traffic necessitates higher capacities in long-haul systems [1]. Mode-division multiplexing (MDM) in multi-mode fiber (MMF), a form of multi-input multi-output (MIMO) transmission, is a promising method to increase per-fiber capacity [2]. In an MMF with D propagating modes, ideally the MIMO channel capacity is D times that of a single mode. However, the MIMO capacity of an MMF is a random variable because of gain and loss variations among modes, collectively referred as mode-dependent loss (MDL), in concert with random mode coupling [3–5]. At any transmission rate, outage may occur with a probability that depends on the statistics of coupled MDL [3,5]. Various encoding schemes may be designed to increase the rate or reduce the outage probability [6], but for any random MIMO channel there is a fundamental tradeoff between achievable rates and outage probabilities known as the *diversity-multiplexing tradeoff* (DMT). In MIMO wireless communications, the DMT was introduced for single-user narrowband Rayleigh fading channels at infinite SNR [7] and generalized to other fading models [8], finite SNR [9], wideband channels [10], and multiuser channels [11]. In this Letter, we study the DMT for MDM in MMF for the first time.

MIMO channels in wireless and MMF media have some similarities, but exhibit fundamental differences that affect the choice of encoding and signal processing methods [12]. Wireless MIMO channels are random because of multipath propagation [12]. By contrast, MMF channels are random because of energy transfer between propagating modes, which is known as *mode coupling* [4]. Mode coupling may be induced by random or intentional perturbations of the MMF or by mode scrambler devices [4]. When mode coupling occurs with approximately equal strength between all modes, and the length over which propagating fields remains correlated is short relative to the system length, signal propagation is said to be in the *strong-mode-coupling regime* [4]. Strong mode coupling is beneficial because it decreases MIMO signal processing complexity [13], reduces nonlinear effects [14], and minimizes the variance of MDL, increasing average channel capacity [3].

Assuming strong coupling, an MMF can be described using K_{sec} independent equal-length sections where $K_{\text{sec}} \gg 1$ [3,4,12]. Neglecting nonlinearity and noise, the propagation operator may be represented by a $D \times D$ matrix multiplying complex baseband modal envelopes at frequency Ω:

$$\mathbf{M}_{\text{tot}}(\Omega) = \exp\left(-\frac{i}{2}\Omega^2\beta_2 L_{\text{tot}}\right) \cdot \prod_{k=1}^{K_{\text{sec}}} \mathbf{V}^{(k)}\Lambda(\Omega)\mathbf{U}^{(k)H}. \quad (1)$$

In the exponential factor in (1), L_{tot} is the total system length and β_2 is the chromatic dispersion constant (mode-dependent chromatic dispersion, typically small, is neglected). In (1), mode-averaged group delay is neglected for simplicity, and mode-averaged loss is assumed to be compensated by optical amplifiers. (In wireless channels, the latter assumption is not valid, since average loss is a random variable governed by the fading statistics.) The latter factor in (1) is a product of three $D \times D$ matrices for each of the K_{sec} fiber sections. In the kth section, $\mathbf{V}^{(k)}$ and $\mathbf{U}^{(k)}$ are random unitary matrices representing mode coupling between sections, and the uncoupled propagation operator is:

$$\Lambda(\Omega) = \text{diag}\left[\exp\left(\frac{g_1}{2} - i\Omega\tau_1\right) \quad \ldots \quad \exp\left(\frac{g_D}{2} - i\Omega\tau_D\right)\right], \quad (2)$$

where the τ_j are uncoupled group delays with $\sum_{j=1}^{D}\tau_j = 0$, the g_j are uncoupled modal gains (measured in log-power or decibel units) with $\sum_{j=1}^{D} g_j = 0$ and $(1/D)\sum_{j=1}^{D} g_j^2 = \sigma_g^2$, and $^{\text{H}}$ denotes Hermitian conjugate. Coupled MDL is characterized by the *spatial subchannel gains* λ_j [3], which are the singular values of $\mathbf{M}_{\text{tot}}(\Omega)$ or, equivalently, the square roots of the eigenvalues of $\mathbf{M}_{\text{tot}}(\Omega)\mathbf{M}_{\text{tot}}(\Omega)^H$.

The dominant noise in long-haul systems is amplified spontaneous emission from optical amplifiers, which is an additive white Gaussian noise over the signal band [15] and, as $K_{\text{sec}} \gg 1$, can be modeled as spatially white [3]. In long-haul systems, the round-trip propagation delay is much longer than the time scale of channel dynamics [12], so feedback of channel state information to the transmitter for optimal beam-forming is not possible. Therefore, the channel capacity at a single frequency is [3]:

$$C_1 = \sum_{j=1}^{D} \log_2\left(1 + \frac{\mathrm{SNR}}{\frac{1}{D}\sum_{k=1}^{D} E\{\lambda_k^2\}}\lambda_j^2\right), \tag{3}$$

where the signal-to-noise ratio SNR is the mode-averaged received signal power divided by the mode-averaged received noise power. In the capacity C_1 and other quantities defined below, the subscript$_1$ denotes a quantity computed for a single-frequency. Similar to [9], we define the SNR factoring out the mode-average channel gain factor $(1/D)\sum_{k=1}^{D} E\{\lambda_k^2\}$ for a fair analysis of the DMT in the low-SNR regime.

The statistics of the capacity are determined by the statistics of the subchannel gains λ_j. At any frequency, the distribution of their logarithms $[\log(\lambda_1^2)\ \cdots \log(\lambda_D^2)]$ is statistically equivalent to the eigenvalue distribution of the summation of two matrices $\xi\mathbf{G} + \kappa_D\xi^2\mathbf{F}$ [16]. The random matrix $\mathbf{G}$ is a zero-trace Gaussian unitary ensemble, corresponding to the summation of independent, identically distributed random matrices from the Central Limit Theorem, while $\mathbf{F} = \mathrm{diag}[-1 \quad 1 + 2/(D-1) \cdots 1]$ is a deterministic unitary matrix [16]. The constant κ_D lies between 1/3 and 1/2 and is found to be $\kappa_D = D/(2D+2)$ [16]. A factor relating uncoupled MDL to coupled MDL is the *accumulated MDL* parameter [3]:

$$\xi = \sqrt{K_{\mathrm{sec}}}\sigma_g. \tag{4}$$

The accumulated rms MDL ξ and the number of modes D are sufficient to characterize the statistics of the λ_j in (3). The rms MDL per section σ_g is sufficient to characterize the statistics of uncoupled MDL per section in (4).

Figure 1 shows the probability density function (PDF) of the single-frequency capacity C_1 for SNR = 9 dB, ξ = 10 dB and for D = 6, 12, 20 and 30 modes, which was obtained by Monte Carlo simulation. The capacity is observed to be approximately Gaussian-distributed, an approximation that becomes more accurate for higher values of D. As expected, the average capacity $C_{\mathrm{avg}} = E\{C\}$ is roughly proportional to D, whereas the variance of the capacity is relatively insensitive to D.

In order to characterize the degrees of freedom of a MIMO channel, the *spatial multiplexing gain* for a given capacity C is defined as [5,9]:

$$r = \frac{C}{\log_2(1+\mathrm{SNR})}. \tag{5}$$

Using (3) and (5), the single-frequency multiplexing gain $r_1 = C_1/\log_2(1+\mathrm{SNR})$ is limited by the number of modes D:

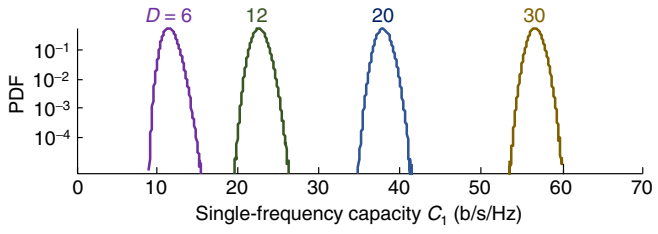

Fig. 1. Distribution of single-frequency capacity C_1 for D = 6, 12, 20, and 30 using 10^7 channel realizations for SNR = 9 dB and ξ = 10 dB.

$$\log_2\prod_{j=1}^{D}\left(1+\frac{\mathrm{SNR}\cdot\lambda_j^2}{\frac{1}{D}\sum_{k=1}^{D}E\{\lambda_k^2\}}\right) \le E\left\{\log_2\prod_{j=1}^{D}\left(1+\frac{\mathrm{SNR}\cdot\lambda_j^2}{\frac{1}{D}\sum_{k=1}^{D}\lambda_k^2}\right)\right\}$$
$$\le E\left\{\log_2\prod_{j=1}^{D}(1+\mathrm{SNR})\right\} = D\log_2(1+\mathrm{SNR}). \tag{6}$$

In (6), the first inequality follows from Jensen's inequality and the second inequality follows from the arithmetic mean–geometric mean inequality with $\prod_{j=1}^{D}\lambda_j^2 = 1$. Note that both inequalities become equalities if and only if $\lambda_1 = \lambda_2 = \cdots = \lambda_D = 1$, i.e., in the absence of MDL.

For a given multiplexing gain and SNR, the outage probability for an instantaneous single-frequency capacity C_1 is:

$$P_{\mathrm{out},1}(r_1, \mathrm{SNR}) = \mathrm{Prob}[C_1 < r_1\log_2(1+\mathrm{SNR})], \tag{7}$$

where $C_{\mathrm{out},1} = r_1\log_2(1+\mathrm{SNR})$ is the single-frequency outage capacity corresponding to a single-frequency outage probability $P_{\mathrm{out},1}(r_1, \mathrm{SNR})$.

We analyze the single-frequency outage probability $P_{\mathrm{out},1}$ as a function of SNR and ξ. Figure 2 shows curves of rms MDL ξ versus single-frequency multiplexing gain r_1 for different outage probabilities for SNR = 9 dB and D = 12 modes. As shown above, $\lim_{\xi\to 0\ \mathrm{dB}} P_{\mathrm{out},1}(r_1 = D, \mathrm{SNR}) = 0$. Hence, the outage probability curves intersect at the point ($r_1 = D, \xi = 0$ dB). From a system design standpoint, Fig. 2 clearly shows the importance of MDL management. For example, for $\xi \sim$ 7–8 dB, r_1 is roughly $D/2$, i.e., only half the available modal degrees of freedom effectively contribute to the transmission rate at acceptable outage probabilities.

Figure 3 shows curves of SNR versus single-frequency multiplexing gain r_1 for different outage probability values for $\xi = 10$ and $D = 12$ modes. Using (3) and $\prod_{j=1}^{D}\lambda_j^2 = 1$, it can be shown that $\lim_{\mathrm{SNR}\to\infty} P_{\mathrm{out},1}(r_1 = D, \mathrm{SNR}) = 0$. Note that this convergence is not observable over the practical range of SNR values in Fig. 3.

As motivated in [7–9] we are interested in the coefficient governing an exponential decrease of outage probability with increasing SNR. For a given outage probability (7), following the finite-SNR definition [10], the *diversity gain* at a single frequency is:

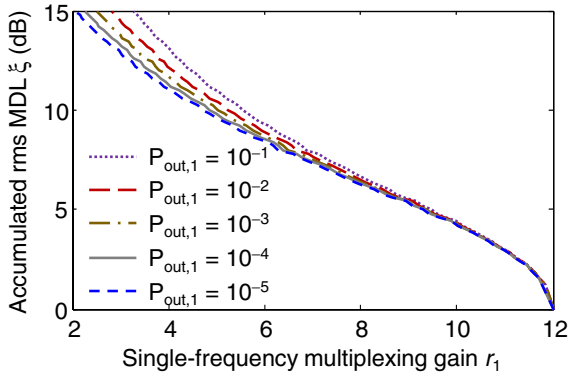

Fig. 2. Accumulated rms MDL ξ versus single-frequency multiplexing gain r_1 using 2×10^7 channel realizations for SNR = 9 dB and D = 12 modes.

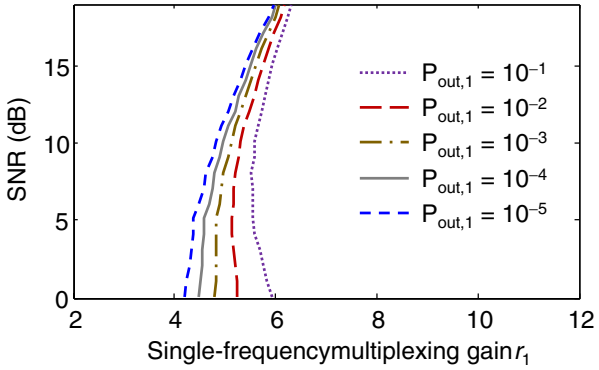

Fig. 3. SNR versus single-frequency multiplexing gain r_1 using 2×10^7 channel realizations for $\xi = 10$ dB and $D = 12$ modes.

$$d_1(r_1, \mathrm{SNR}) = -\frac{\partial \log(P_{\mathrm{out},1}(r_1, \mathrm{SNR}))}{\partial \log(\mathrm{SNR})}. \tag{8}$$

The diversity gain $d_1(r_1, \mathrm{SNR})$ at a given value of SNR governs the scaling of the single-frequency outage probability in proportion to $\mathrm{SNR}^{-d_1(r_1,\mathrm{SNR})}$.

Figure 4 shows the single-frequency diversity gain $d_1(r_1, \mathrm{SNR})$ for various values of the single-frequency multiplexing gain r_1, which has been computed numerically for the parameters in Fig. 3. For any encoding scheme, the upper boundary of the achievable region of operation is limited by these diversity gain curves. As an example, the maximum achievable diversity gains are $d_1 = 4$ for SNR = 8 dB and $r_1 = 4.5$; $d_1 = 1.1$ for SNR = 8 dB and $r_1 = 5$; $d_1 = 5.2$ for SNR = 9 dB and $r_1 = 4.5$; and $d_1 = 1.6$ for SNR = 9 dB and $r_1 = 5$.

Thus far we have focused on the single-frequency DMT. For an MMF channel in the strong-coupling regime, MDL is frequency dependent, with a coherence bandwidth of the order of the reciprocal of the coupled rms delay spread [17]. If a wideband signal occupies a bandwidth much larger than the coherence bandwidth, *frequency diversity* reduces the variance of the capacity and thus reduces the outage probability for the wideband signal. The difference between the average and outage capacities for a given outage probability is characterized by a *frequency diversity order* [17]:

$$F_D \approx [(C_{\mathrm{avg}} - C_{\mathrm{out},1})/(C_{\mathrm{avg}} - C_{\mathrm{out},F_D})]^2, \tag{9}$$

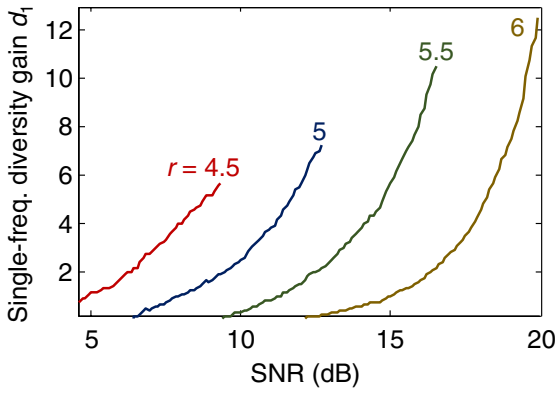

Fig. 4. Single-frequency diversity gain $d_1(r_1, \mathrm{SNR})$ versus SNR for different values of single-frequency multiplexing gain r_1 using 2×10^7 channel realizations for $\xi = 10$ dB and $D = 12$ modes.

where $C_{\mathrm{out},1}$ is the single-frequency outage capacity and C_{out,F_D} is the wideband outage capacity at diversity order F_D [17]. The diversity order F_D can be computed from a correlation matrix of samples of the frequency-dependent coupled subchannel gains λ_j [17], and is approximately the coupled rms delay spread normalized by the symbol interval.

In order to analyze the impact of frequency diversity on the DMT, we approximate the distribution of capacity as Gaussian, which is justified empirically in Fig. 1. Using a tail probability approximation [18] valid for low outage probabilities:

$$P_{\mathrm{out},1} \approx \exp(-(C_{\mathrm{avg}} - C_{\mathrm{out},1})^2/\sigma_C^2)/12, \tag{10}$$

$$P_{\mathrm{out},F_D} \approx \exp(-(C_{\mathrm{avg}} - C_{\mathrm{out},F_D})^2 F_D/\sigma_C^2)/12. \tag{11}$$

Note that (10) and (11) are consistent with (9) for $P_{\mathrm{out},1} = P_{\mathrm{out},F_D}$. Generalizing (8):

$$d_{F_D}(r_{F_D}, \mathrm{SNR}) = -\frac{\partial \log(P_{\mathrm{out},F_D}(r_{F_D}, \mathrm{SNR}))}{\partial \log(\mathrm{SNR})}. \tag{12}$$

For a given SNR and for $r_1 = r_{F_D} = r$ (i.e., $C_{\mathrm{out},1} = C_{\mathrm{out},F_D}$), excluding a constant term, we have $\log(P_{\mathrm{out},F_D}(r, \mathrm{SNR})) \propto [C_{\mathrm{avg}} - (r \log_2(1 + \mathrm{SNR}))]^2 F_D$. Moreover, as shown in [17], F_D is almost independent of SNR. Therefore, we obtain:

$$d_{F_D}(r, \mathrm{SNR}) \approx F_D \cdot d_1(r, \mathrm{SNR}). \tag{13}$$

In other words, for a given multiplexing gain, the diversity gain increases approximately in proportion to the diversity order.

Lastly, we compare the DMTs for MIMO channels in wireless and MMF media. For a wireless MIMO channel with D transmit and D receive antennas, assuming Rayleigh fading, as $\mathrm{SNR} \to \infty$, the asymptotic single-frequency diversity gain is $(D - r)^2$ [7]. For finite values of SNR, the diversity gain is reduced, as studied in [9]. In the case of a frequency-selective wideband channel, the asymptotic diversity gain is $(LD - r)(D - r)$, where L is the channel delay spread normalized by the symbol interval [10]. When $LD \gg r$, the diversity gain scales roughly in proportion to the delay spread. For a MMF MIMO channel with D propagating modes, as $SNR \to \infty$, the asymptotic multiplexing gain is D. For finite values of SNR, values of the single-frequency diversity gain are comparable to those in wireless MIMO channels. In the wideband regime, the diversity gain scales roughly in proportion to the frequency diversity order for low outage probabilities, hence it is approximately proportional to the coupled rms delay spread normalized by the symbol interval.

In conclusion, we have studied the DMT for MIMO channels in MMF for the first time. We have investigated the tradeoff for $D = 12$ modes, studying the effects of signal-to-noise ratio, mode-dependent loss, and frequency diversity order. The DMT may provide insights aiding the design of capacity-approaching encoding schemes for MDM systems.

Discussions with Prof. Ayfer Özgür are gratefully acknowledged. This research was supported by National Science Foundation Grant Number ECCS-1101905, Corning, Inc., and a Stanford Graduate Fellowship.

References

1. R. J. Essiambre and R. W. Tkach, Proc. IEEE **100**, 1035 (2012).
2. T. Morioka, Y. Awaji, R. Ryf, P. J. Winzer, D. Richardson, and F. Poletti, IEEE Commun. Mag. **50**(2), 31 (2012).
3. K.-P. Ho and J. M. Kahn, Opt. Express **19**, 16612 (2011).
4. K.-P. Ho and J. M. Kahn, in *Optical Fiber Telecommunications VI*, I. P. Kaminow, T. Li, and A. E. Willner, eds., (Elsevier, 2013), pp. 491–568.
5. P. J. Winzer and G. J. Foschini, Opt. Express **19**, 16680 (2011).
6. P. Elia, K. R. Kumar, S. A. Pawar, P. V. Kumar, and H. Lu, IEEE Trans. Inf. Theory **52**, 3869 (2006).
7. Z. Lizhong and D. Tse, IEEE Trans. Inf. Theory **49**, 1073 (2003).
8. L. Zhao, W. Mo, Y. Ma, and Z. Wang, IEEE Trans. Inf. Theory **53**, 1549 (2007).
9. R. Narasimhan, IEEE Trans. Inf. Theory **52**, 3965 (2006).
10. A. Medles and D. Slock, in *Proceedings of IEEE International Symposium on Information Theory* (IEEE, 2005), pp. 1813–1817.
11. D. Tse, P. Viswanath, and L. Zheng, IEEE Trans. Inf. Theory **50**, 1859 (2004).
12. S. Ö. Arik, J. M. Kahn, and K.-P. Ho, IEEE Signal Process. Mag. **31**(2), 25 (2014).
13. S. Ö. Arik, D. Askarov, and J. M. Kahn, J. Lightwave Technol. **31**, 423 (2013).
14. S. Mumtaz, R. Essiambre, and G. Agrawal, J. Lightwave Technol. **31**, 398 (2013).
15. R. J. Essiambre, G. Kramer, P. J. Winzer, G. J. Foschini, and B. Goebel, J. Lightwave Technol. **28**, 662 (2010).
16. K.-P. Ho, J. Lightwave Technol. **30**, 3603 (2012).
17. K.-P. Ho and J. M. Kahn, J. Lightwave Technol. **29**, 3719 (2011).
18. C. Marco, D. Dardari, and M. K. Simon, IEEE Trans. Wirel. Commun. **2**, 840 (2003).